



Enhancing the sustainability of high strength concrete in terms of embodied energy and carbon emission by incorporating sewage sludge and fly ash

Mithesh Kumar¹ · Shreelaxmi Prashant¹ · Muralidhar V. Kamath¹

Received: 2 February 2022 / Accepted: 14 April 2022 / Published online: 18 May 2022
© The Author(s) 2022

Abstract

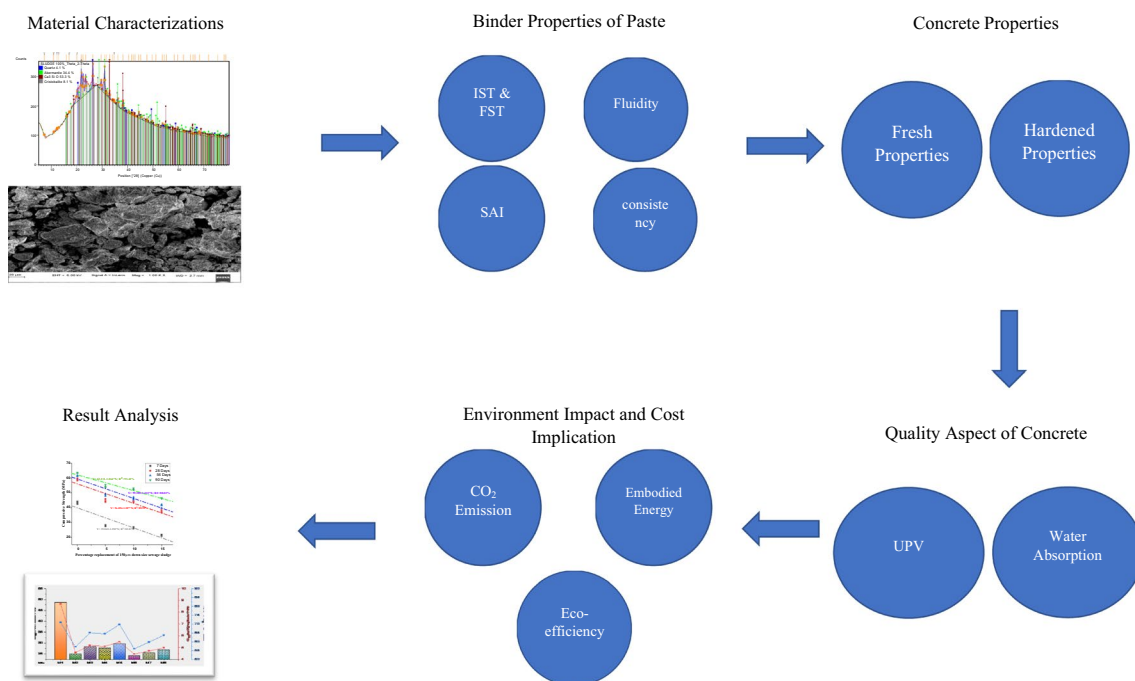
This paper discusses the properties of dried sewage sludge (SS) and its influence on the microstructure development of HVFA concrete when used as a partial replacement of binder material. A detailed characterization of dried sludge samples collected from a sewage treatment plant is carried out using XRF, XRD, TGA, and FTIR techniques. HVFA concrete mix is designed for 50 MPa with 50% fly ash of the total binder content. Sludge is ground to a particle size of 150 μ and 75 μ and replaced at levels of 5%, 10%, and 15% of the total binder content. The strength activity index of the dried sludge sample is acceptable as per standards. Taking concrete mixes with HVFA as a reference, the fresh properties of binder paste and concrete with sewage sludge have been studied. Mechanical properties that define the applicability to various infrastructure projects are reported for all the studied mixes. EI, CI, COST per unit compressive strength for all mixes are also determined to comment on the environmental impact of the use of SS in concrete. The compressive strength of concrete specimens decreases with the increase in replacement level of SS. However, in comparison with OPC concrete, 75 μ m SS at 5% replacement level concrete mechanical strength is within the acceptable limit for M50 concrete mix. The addition of SS as a binder to the concrete has a lower environmental impact, embodied energy, CO₂ emission, and cost per unit strength. But more than 10% replacement level resulted in reducing CS, FS, and STS by 11.17%, 6.23%, and 6.99%.

✉ Shreelaxmi Prashant
shreelaxmi.p@manipal.edu

Mithesh Kumar
kumar.mithesh@gmail.com

¹ Department of Civil Engineering, Manipal Institute of Technology, Manipal Academy of Higher Education, Manipal, India

Graphical abstract



Keywords Sewage sludge · High volume fly ash concrete · Mechanical properties · Carbon footprint · Embodied energy

Abbreviations

CO ₂	Carbon dioxide
CE	Carbon emission
CI	Carbon emission index
CS	Compressive strength
EE	Embodied energy
EI	Embodied energy index
FESEM	Field emission scanning electron microscope
FST	Final setting time
FS	Flexural strength
FA	Fly ash
FTIR	Fourier transform infrared spectroscopy
GHG	Greenhouse gas
HVFA	High-volume fly ash
HVFAC	High volume fly ash concrete
IST	Initial setting time
COST	Material cost index
MoE	Modulus of elasticity
MSWA	Municipal solid waste ash
MWWTP	Municipal waste water treatment plant
OPC	Ordinary Portland cement
PC	Portland cement
SS	Sewage sludge
SSA	Sewage sludge ash
STS	Split tensile strength
SAI	Strength activity index

SCMs	Supplementary cementitious materials
SDG	Sustainable development goals
TGA	Thermo gravimetric analysis
UPV	Ultrasonic pulse velocity
WA	Water absorption
XRD	X-ray powder diffraction
XRF	X-ray fluorescence

Introduction

The sustainability of concrete depends on the amount of CO₂ and other GHGs emitted in the production and procurement of raw materials, mixing, casting, and curing. Due to globalization and increased population, industrial waste disposal is one of the most significant challenges humankind is facing. In this context, attempts are being made to reduce carbon emissions in concreting through the effective utilization of industrial by-products. Sustainable development goals (SDG) and standards have suggested using waste materials/by-products that reduce carbon emission and embodied energy.

Cement production is an energy-intensive process. As of now, 4400 million tons of cement are manufactured yearly worldwide. It is also anticipated that the number will rise to over 5500 million tons by 2050. About 8% of the

world's CO₂ emission is attributed to cement production. India stands at the second position in cement production and cement-related CO₂ emissions. Cement production in India is estimated to rise to 3000 MT, emitting nearly 1.3 billion tons of CO₂ by 2050 [1]. The CO₂ emissions are found to reduce with SCMs in one of the binder phases. Approximately 13–22% of CO₂ emissions were reduced by SCMs depending on the level of replacement used [2]. O'Brien et al. (2009) reported that the primary source of GHG emissions is the concrete industry. Seven percent of the global GHG emissions are from PC production. In addition, the cement industry releases gases such as SO₂ and NO_x that can cause environmental degradation and other associated effects [3, 4].

Many researchers have unanimously accepted that FA reduces GHG emissions when replaced with Portland cement [5]. The reduction in GHG emissions depends on the source and condition of raw materials, the type of supplementary cementitious material used, the percentage of replacement level, and the transportation distance. Industrial by-products, such as FA and slag, are widely used and accepted as partial replacements to OPC [6]. The effective use of improperly disposed of municipal and industrial by-products/wastes can reduce pollution and result in the sustainable use of natural resources [7]. Many experimental investigations are performed on using other wastes in concrete, such as palm oil fuel ash, rice hush ash, MSWA, incinerated bottom ash, agro-waste, and SSA, as a part of cementitious binder in concrete production [8–22].

Due to the ever-increasing energy demand, many thermal power plants were set up across the globe, resulting in the large-scale production of FA as a by-product. Therefore, the safe disposal of FA to prevent environmental pollution has become a global challenge. FA can be used as a valuable resource in concrete, greenhouse gas emissions, and embodied energy. HVFA is an approach to maximize the FA content in concrete and minimize OPC use for a similar level of mechanical properties. In contrast, Dunstan et al. (1992) referred to any concrete containing more than 40% of FA as HVFA concrete. Many experimental investigations have recommended 30–70% cement replacement by FA for concrete having 28 days strength of 40–50 MPa [3, 23–33].

Sivasundaram et al. (1990) observed the strength development of HVFA concrete over three years. Concrete gained strength of 70 MPa and modulus of elasticity of 47 GPa with prolonged curing for two years [34]. Jiang and Malhotra (2000) recommended the use of a large amount of FA as binders (55%) in conjunction with the use of superplasticizers to achieve higher slumps of 100 mm and above since HVFAC is associated with a low W/B [32]. Bouzoubaa et al. (2000) found improvement in resistance to chloride ion penetration characteristics with HVFA blended cement. Further, it was also noticed that the performance of

HVFA against chloride ion penetration was enhanced with an increase in the inter-grinding time of binder material [35].

SS is a by-product of the MWWTP. The estimated dry sludge production quantities annually are 8910, 6510, 3955, 2960, 650, 580, 550, and 370 thousand metric tons EU-27, USA, India, China, Iran, Turkey, Canada, and Brazil, respectively [36–39]. Presently, in India, out of the 62,000 MLD sewage generated, only 20,120 MLD goes into the treatment plant. The quantity of dry sludge generated in India is expected to increase many times due to the extensive installation of municipal sewage treatment plants under the Swachh Bharat Mission [31–33]. Due to large SS production, a proper disposal strategy is essential to manage dried sludge quantities. Various disposal strategies like agricultural manure, fillers in landscapes, gardening, and all the unused SS get dumped into the landfills. With the lack of land spaces and new environmental regulations, it is essential to explore new applications of SS [40, 41]. There is a need for efficient recycling, resource recalcination, and proper SS treatment [42]. Several researchers identified the presence of calcium, silica, and alumina phases in SS on analysis of its chemical composition. SS is found to possess properties similar to popular pozzolanic material used in concrete [43, 44].

Marisal et al. (2004) investigated the mechanical properties of concrete specimens containing treated plant sludge and recommended replacing levels up to 10% of binder content [45]. Baskar et al. (2006) have successfully replaced 9% of the binder with sludge obtained from the residue of the textile industry and wastewater in clay bricks. At a 9% replacement level, the brick samples satisfied the requirement of the BIS for compressive strength, weight loss, and shrinkage parameters [46]. Patel and Pandey (2009) reported that the sludge from the textile industry had a potential for reuse as construction materials [47]. Jamshidi et al. (2010) replaced cement with dry sludge at 0%, 5%, 10%, 20%, and 30% in concrete. The sizing and milling of dry sludge to a finer particle size can improve the mechanical properties of concrete any unreacted particles are left to act as a filler in concrete [48].

The dried sludge organic content limited to 13% can be used as an additive to mix. The increase in sludge by more than 5% was adversely affected workability [45–47]. Similar results have been found for both wet and dry wastewater sludge used in concrete.

The current study investigates the physical and chemical properties of FA and SS as a binder material. The fresh and hardened properties of concrete mixes at different levels of replacement of SS are reported. The higher the energy required to produce raw material, the higher the energy cost, resulting in higher CO₂ emissions to the atmosphere and embodied energy. All these would result in higher CO₂ emission and embodied energy, creating a higher negative

impact on the environment. This study performs CE and EE of the binding material and concrete mixes at a different replacement level.

Experimental program

Materials

Binder material

OPC Forty-three Grade confirming IS 8112-2013 [49] is used for the study. Low calcium FA (Class F) was procured from a Raichur, Karnataka, India. Dried SS was collected from the dry sludge bed at the MWWTP at End Point, MAHE, Manipal, Karnataka, India, and dried for seven more days in sunlight to remove excess moisture.

After oven-drying at 105 °C for 24 h, the sludge was ground for 1 h in a ball mill. The ground residue was sieved through 150 and 75-micron meter IS standard sieves and collected separately. The particle size analysis of all the ingredients going into the binder system is illustrated in Fig. 1. The properties of various binder materials used in the present study are presented in Tables 1 and 2.

Chemical analysis with X-ray fluorescence Semi-chemical quantitative analysis of the oxides is performed, and the outcomes are tabulated in Table 2. Sewage sludge comprises SiO_2 , Al_2O_3 , Fe_2O_3 , CaO , Na_2O , and P_2O_5 , which is quite similar to FA. The proportions of SiO_2 and Al_2O_3 , which are the main reactive components responsible for pozzolanic reactions in the binder system (ASTM C125, 2007), are lower than FA. Sludge is composed primarily of quartz

Table 1 Physical characteristics of raw materials

Physical characteristics	Cement	FA	SS (150 μm)	SS (75 μm)
Specific gravity	3.12	2.32	1.95	2.13
Specific surface area (m^2/g)	0.313	0.377	0.320	0.315
Particle size	D10	3.68	2.17	5.27
	D50	14.85	8.72	35.13
	D90	32.32	27.99	78.45

and calcite. The same is noted by Valls et al. (2004) [45]. Clay is absent in dry sludge, which signifies the absence of a stable binder phase on hydration. However, it can be used as a partial replacement for cement. The range in which various compounds are present in the sludge presented in previous research articles is also listed in Table 2. The ternary representation of SiO_2 - CaO - Al_2O_3 - Fe_2O_3 concerning that of OPC, FA, and SS is presented in Fig. 2.

X-ray powder diffraction (XRD) of SS XRD spectra of SS are presented in Fig. 3. The crystalline phases of the SS mainly consist of quartz SiO_2 4.1%, Akermanite 34.4%, Ca_3SiO_5 53.3%, and Cristobalite 8.1%.

Thermogravimetric analysis of sewage sludge The result of TGA is presented in Fig. 4. The SS sample tested was found to have undergone thermal degradation in two phases. The first phase of primary degradation occurred at the temperature range of 100–500 °C, wherein the sludge sample was found to experience a high rate of mass loss. In the second phase, continuous decomposition of SS occurs at a

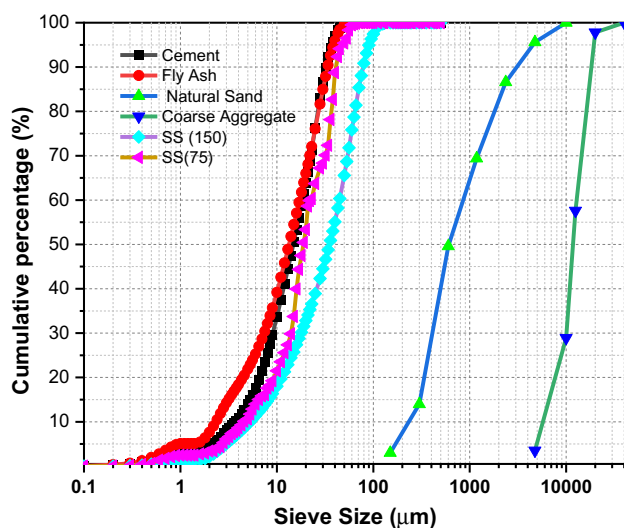


Fig. 1 Particle size distribution of concrete ingredient

Table 2 Chemical composition of binder materials

Composition	OPC	FA	SS (%)	SS observed value in literature	
				Min	Max
SiO_2	20.27	53.25	12.013	2.06 [50]	42.54 [51]
Al_2O_3	8.98	25.62	4.424	2.06 [50]	14.79 [52]
Fe_2O_3	3.71	6.4	41.715	4.58 [50]	49.35 [53]
CaO	59.21	4.7	8.985	2.40 [52]	22.70 [45]
MgO	1.85	1.04	0.014	0.01 [15]	5.78 [27]
P_2O_5	—	—	23.302	5.00 [54]	22.55 [27]
Na_2O	0.15	2.22	6.247	0.31 [55]	1.11 [50]
K_2O	0.98	0.87	2.122	0.53 [55]	6.19 [27]
TiO_2	1.35	—	1.069	0.52 [52]	3.42 [50]
SO_3	2.52	1.29	—	0.0 [48, 51, 52, 56]	9.57 [27]
Cl^-	—	—	—	0 [50, 53, 57]	0.5 [55]
LOI	1.47	2.85	48.59	47.50 [50]	73.40 [50]

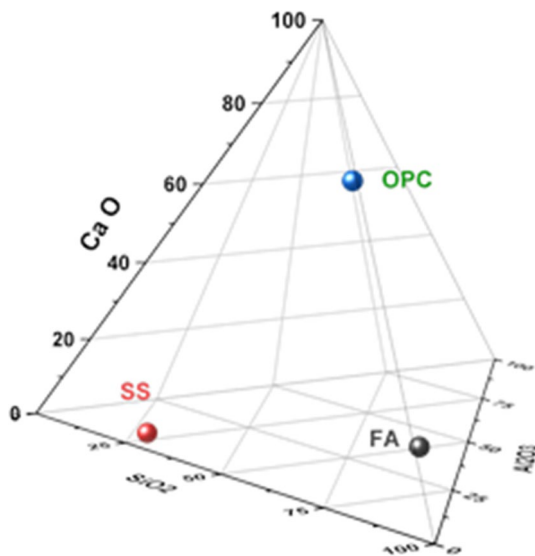


Fig. 2 Ternary 3D plot of binder materials

high temperature of 500–900 °C with a comparatively lower mass-loss rate.

Fourier transform infrared spectroscopy of sewage sludge FTIR analysis was carried out for SS using JASCO FTIR-6300 with a wavelength range of 400–4000 cm^{-1} results which are shown in Fig. 5. Inorganic bonded O–H groups with a wavenumber of 3250 cm^{-1} are observed. The broad peak at the 3600–4000 cm^{-1} region signifies the presence of O–H and N–H functional groups. Hence, alcohols,

acids, amides, and amines are also noted. Multiple peaks indicate the presence of C–H groups in the 1042–2925 cm^{-1} region. The primary absorbance in FTIR spectra in the region 450–1050 cm^{-1} is due to the Si–O bond of silicate impurities and traces of clay minerals.

Microstructure The FESEM images of OPC, FA, and SS are shown in Fig. 6. From the FESEM image of SS, it is observed that the particle sizes appear to be more prominent than FA. SS appears crystalline in nature. It consists of the random orientation of solids with irregular shapes and sizes. Therefore, to attain higher reactivity, it is essential to grind the SS to a finer level.

Aggregates

Natural river sand and gravel as fine and coarse aggregate in accordance with IS 383-1970 1970 (Reaffirmed 2011) are used for the present study. Table 3 and Fig. 1 show aggregates physical properties and sieve analysis.

Superplasticizer

High range water reducing agent Rofluid H1 (PCE base), with a specific gravity of 1.15 and pH of 4.5, was used in all mixes to enhance the workability of concrete. The chloride ion and alkaline percentages are ≤ 0.1 and 0.4, respectively.

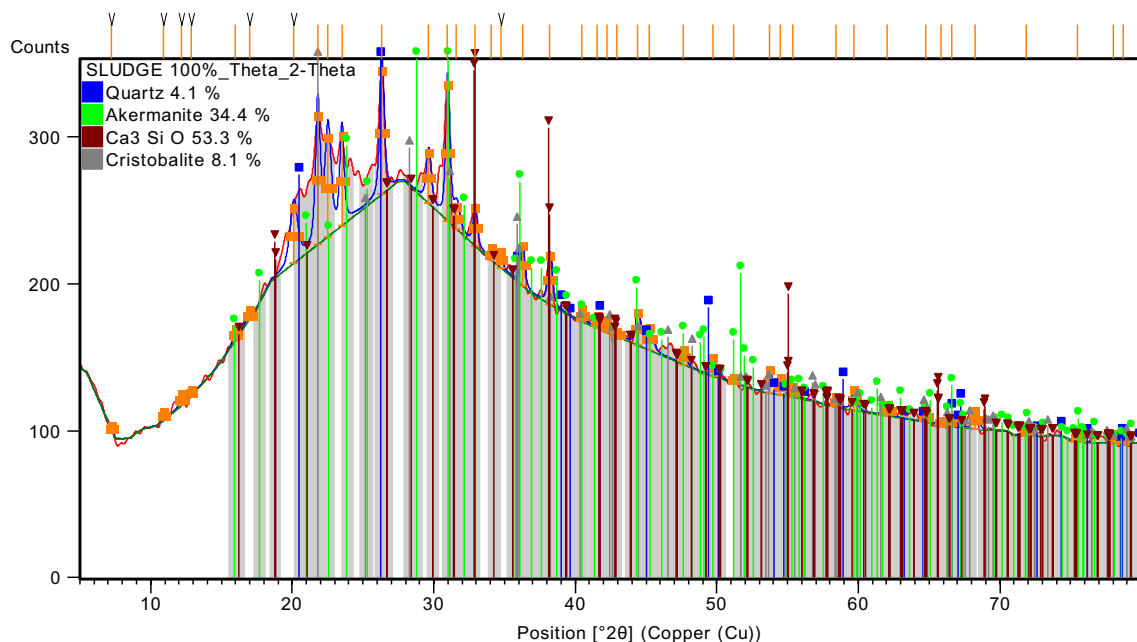


Fig. 3 XRD pattern of sewage sludge

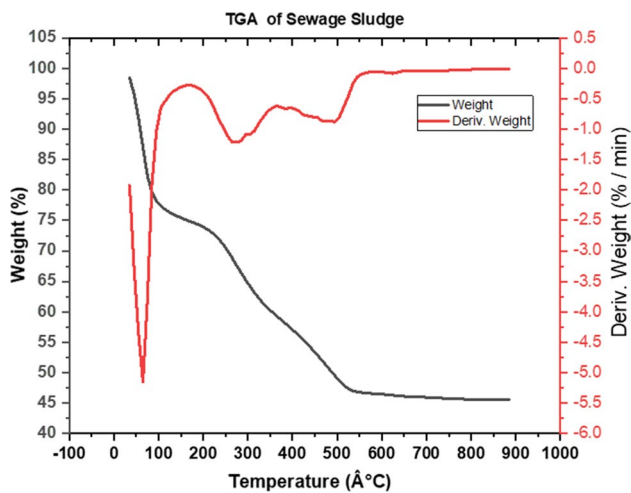


Fig. 4 The TGA of raw SS

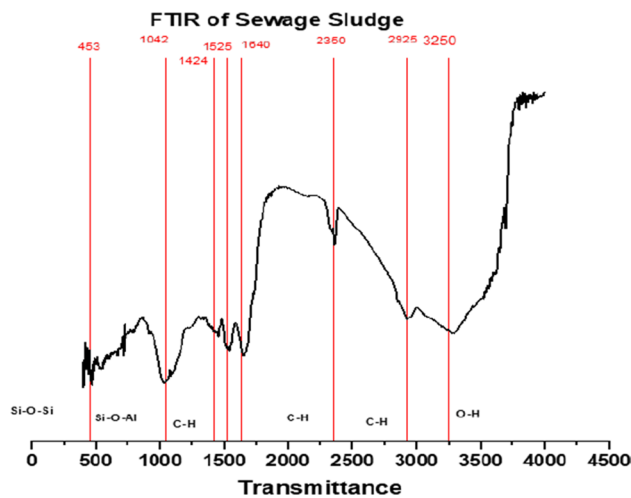


Fig. 5 FTIR spectra of sewage sludge

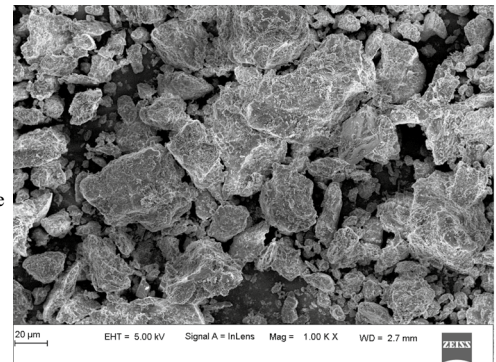
Preparation of the paste

The mix proportions of various combinations of binder blends used for the study are listed in Table 4. The blended binder paste was carried out as per the norms stipulated in EN 196-3 [58].

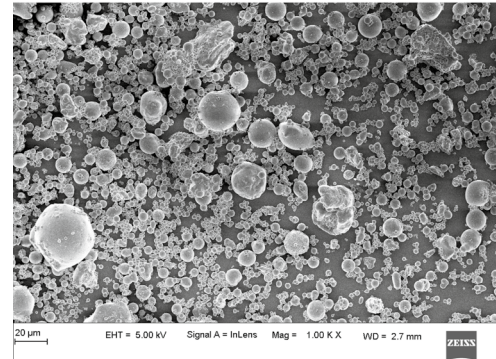
Mix proportioning

The mix proportions used for the current investigation are presented in Table 5. Sewage sludge was replaced at 5%, 10%, and 15% of the total binder content. Physical and mechanical properties of HVFA high strength concrete with three levels of sludge replacement were investigated through experimental procedures. Using the Department of Environment's Design (DOE) method, M50 concrete is designed with 50% cement and 50% FA as a binder. The w/b ratio of

Sewage Sludge



Fly ash



OPC

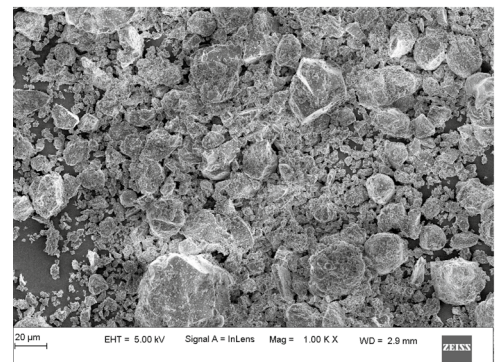


Fig. 6 Microstructure of sewage sludge, fly ash, and OPC

Table 3 Properties of natural aggregates

Properties	Coarse aggregate	Fine aggregate
Specific gravity	2.65	2.55
Bulk density (Loose state) (kg/m ³)	1428	1454
Bulk density (compacted state) (kg/m ³)	1679	1645
Water absorption (%)	0.42	0.85
Silt content (%)	—	1.50
Bulking of sand (%)	—	25

0.3 is used for all the mixes. After casting, the specimens are de-molded after 24 h and then immersed in water for curing as per IS 10086-2008 [59].

Table 4 Mix designation for blended mixes

Blends	Combination	General designation	Binder content		
			OPC (%)	FA (%)	SS (%)
Control	OPC	C	100	–	–
Binary blends	OPC + FA	CF	50	50	–
Ternary blends	OPC + FA + SS (150 μ m)	CFS150-5	47.5	47.5	5
		CFS150-10	45	45	10
		CFS150-15	42.5	42.5	15
	OPC + FA + SS (75 μ m)	CFS75-5	47.5	47.5	5
		CFS75-10	45	45	10
		CFS75-15	42.5	42.5	15

Table 5 Mix proportion of concrete used in present study

Mix designation	OPC (kg/m ³)	FA (kg/m ³)	SS-150 μ m (kg/m ³)	SS-75 μ m (kg/m ³)	Sand (kg/m ³)	Coarse aggregate	Water (kg/m ³)	W/B ratio	SP (%)
M1	577	–	–	–	899.94	798.06	191	0.33	1.0
M2	288	288.5	–	–	899.94	798.06	191	0.33	2.1
M3	274.075	274.075	28.85	–	899.94	798.06	191	0.33	2.1
M4	259.65	259.65	57.7	–	899.94	798.06	191	0.33	2.1
M5	245.225	245.225	86.55	–	899.94	798.06	191	0.33	2.1
M6	274.075	274.075	–	28.85	899.94	798.06	191	0.33	2.1
M7	259.65	259.65	–	57.7	899.94	798.06	191	0.33	2.1
M8	245.225	245.225	–	86.55	899.94	798.06	191	0.33	2.1

Specimen casting and curing

OPC, FA, and SS were mixed thoroughly to obtain uniform binder mix. The aggregates are mixed with binders for 2 min to obtain a uniform dry mix. Uniform concrete mix was obtained by continuing the mixing for 2–3 min after water dispersion, and chemical admixture was poured. Later, concrete was cast into specific molds. The molded samples were kept in laboratory conditions for 24 ± 0.5 h and de-molded, later stored in a curing tank in the conventional method for the required durations [60–62].

Experimental procedure

Test on binder material

The setting time of the binder was determined as per the procedure prescribed in ASTM C191 [63]. Standard consistency of binder pastes is performed as per ASTM C187-16 [64]. SAI test was performed according to ASTM C618-05 [65] to study the pozzolanic activity of the binder mix. The fluidity of binder paste was measured (mini-slump flow) as per ASTM C1437 [66].

Tests on concrete

"Compressive strength test has been performed at 7, 14, 28, 56, and 90 days of the curing period using 150 mm cubic size, as per the Indian Standard Specifications IS:516-1959 [60]. The loading rate of 14 N/mm²/min was maintained using CTM of capacity 3000 kN. The split tensile strength was determined as per IS 5816-1999 [67] using specimen sizes of 150 mm diameter and 300 mm height at 7, 28, 56, and 90 days. The rate of load application was within the range of 1.2–2.4 N/mm²/min. The flexural strength test was performed using the prism of size 100 \times 100 \times 500 mm as per IS 516-1959 [60]. Modulus of elasticity (MoE) has been conducted as per IS 516-1959 [60] on the cylinder specimen of size 150 mm diameter and 300 mm height after 28 days of curing. Deformation of the sample under compressive load was found using compressometer and linear variable differential transformer (LVDT) equipment. The ultrasonic pulse velocity (UPV) test was performed as per IS 13311-1-1992 [68] using a TICO Ultrasonic instrument supplied by PROCEQ SA, Switzerland. A water absorption test has been conducted on 150 mm cube specimens following the specifications prescribed in BS 1881-122-1983 [69]. Details of the tests and the corresponding codes referred are mentioned in Table 6 [62].

Table 6 Summary of experimental tests conducted

Sl. no	Tests	Specimen	Standards
1	Setting time	Binder paste	ASTM C191 [63]
2	Standard consistency	Binder paste	ASTM C187-16 [64]
3	Fluidity (Mini-Slump Flow)	Binder paste	ASTM C1437 [66]
4	Strength activity index test	Binder mortar	ASTM C618-05 [65]
5	Slump flow	Concrete	IS 1199-1959 [70]
6	Density	Concrete	BS 1881-114:1983 [71]
7	Compressive strength	Concrete	IS 516-1959 [60]
8	Splitting tensile strength	Concrete	IS 5816-1999 [67]
9	Flexural strength	Concrete	IS 516-1959 [60]
10	Modulus of elasticity	Concrete	IS 516-1959 [60]
11	Ultrasonic pulse velocity	Concrete	IS 13311-1-1992 [68]
12	Water absorption	Concrete	BS 1881-122-1983 [69]

Table 7 Setting time, consistency, and slump flow of binder paste

Binder mix	Setting time		Consistency (%)	Slump flow (mm)
	IST (min)	FST (min)		
C	150	265	31	180
CF	185	305	34	195
CFS150-5	220	335	38	162
CFS150-10	235	350	40	157
CFS150-15	255	375	41	151
CFS75-5	200	315	41	172
CFS75-10	185	330	46	166
CFS75-15	175	360	53	161

Results and discussion

Initial and final setting time

The IST and FST of pastes tested are presented in Table 7. IST and FST vary from 155 to 255 and 265 to 375, respectively. It is noticed that with an increase of SS, the setting time also increases for the pastes containing both 150 μm and 75 μm downsized dried sludge. However, the paste samples containing 75 μm downsized SS have exhibited acceptable setting times at 5% and 10% replacement levels. Mirza et al. (2002), Duran-Herrera et al. (2011), and Huang et al. (201) reported an increase in IST and FST of cement paste with the inclusion of SCMs [25, 72, 73].

Standard consistency of binder

The standard consistencies of binder pastes studied at different replacement levels are shown in Table 7. The consistency value of FA blended cement paste at 50% cement replacement level is 34%, while the control sample consistency

was 31%. A similar trend was observed by Marthong and Agrawal (2012) [74]. Replacement of SS resulted in an increase in the consistency values of the blended pastes due to the higher powder volume and porous and crystalline nature of SS. It is also noted from Table 7 that the consistency value is higher for binder paste with 75 μm downsize SS particle compared to 150 μm downsize at the same replacement level.

Fluidity (mini-slump flow) of binder

The fluidity of various paste compositions studied with and without sludge replacement is presented in Table 7. The slump flow values of the paste mixes were found to range from 151 to 195 mm compared to the slump value of 180 mm for OPC. It is observed that the fluidity of the OPC paste was found to have increased on replacing OPC with 50% FA. However, with the incorporation of SS into the binder, the fluidity is considerably reduced. The SS particles are porous and irregular in shape, hence, more susceptible to water absorption on particle surfaces [75]. Also, the size of SS was found to influence the fluidity.

Strength activity index

The SAI test was conducted to evaluate the pozzolanic activity of SS and presented in Fig. 7. According to ASTM C618-05 [65], the substitutive material is designated a pozzolan if it achieves a 75% of the strength gained by OPC mortar at 7, 14, 28, 56, and 90 days, respectively, with 20% cement replacement. According to the results of the SAI, SS (75 μm) exhibits moderate pozzolanic activity. It can also be seen from the figure that the SAI of SS increased as the curing day advances. The presence and quantities of amorphous phases in the pozzolan contribute to pozzolanic when used as partial replacement to cement.

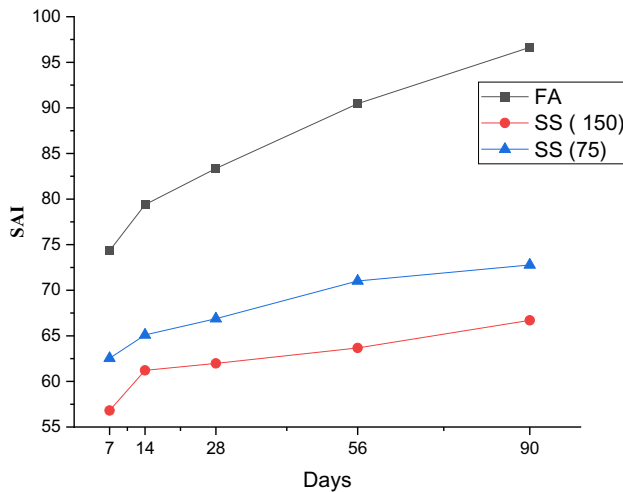


Fig. 7 Strength activity index of supplementary cementitious materials

In comparison, SS has proven to possess lower SAI than FA. Finer grinding may be used for improving pozzolanic activity. In the present study, SS with a particle size of 75 μm possesses moderate pozzolanic activity, suitable to be used as SCM's.

Influence of sewage sludge on slump flow

The slump flow values of freshly mixed concrete mix are illustrated in Fig. 8. A higher slump value is observed in mix M2 because of a higher proportion of FA compared to the OPC (M1) mix. Sahmaran and Yaman (2007) also reported that OPC replacement with 50% FA increased the slump flow by 23.2% [76]. The increase in the percentage

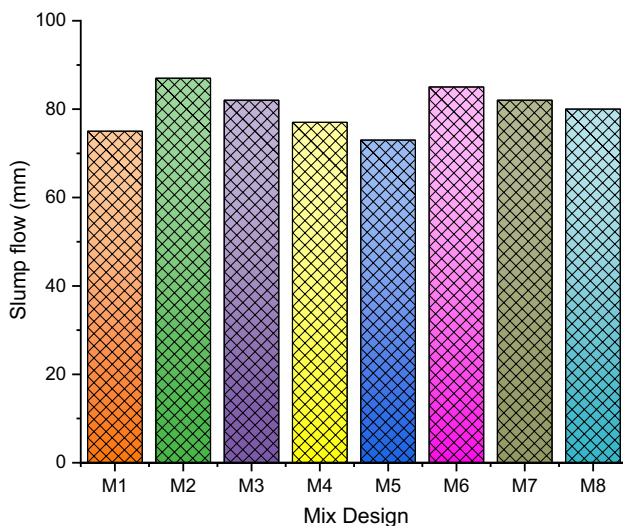


Fig. 8 Slump flow of the concrete mix

replacement of SS resulted in a decrease in slump value for the concrete in both 75 and 150 μm size particles. Similar results are observed by Jamshidi et al. (2011) [48], Ghada Mourtada et al. (2016) [74], and Ehab et al. (2019) [77].

Concrete density

The 28-day concrete density was determined according to BS 1881: Part 114:1983 [71] (Method of determination of density of hardened concrete) [71] and presented in Fig. 9. The density of specimens increased with curing age. Continuous hydration and pozzolanic action from binder materials resulted in dense microstructure at a later age. Compared to the control sample, the concrete density began to drop in addition to 5% of SS. Based on the results obtained, it can be noted that the concrete density decreased with an increase in SS particle size. The same trend was observed by Amminudin et al. (2020) [56]. It is important to note that the addition of FA to the mix lowers the fresh concrete density. The lower specific gravity of FA and SS compared to OPC accounts for a decrease in density. The same trend is observed in studies reported earlier [3, 23, 78]. The deadweight of the structural element is reduced due to a reduction in the density of concrete. So, the use of SS in the binder system can be considered one of the advantages.

Compressive strength

The CS test was performed on concrete samples at 7, 14, 28, 56, and 90 curing days. The measurement of CS of the concrete sample with variable SS content is shown in Table 8. The replacement of 150 μm downsized SS at 5%, 10%, and 15% resulted in a decrease in 28 days strength by 24.12%, 25.54%, and 36.54%, respectively. Whereas 75 μm

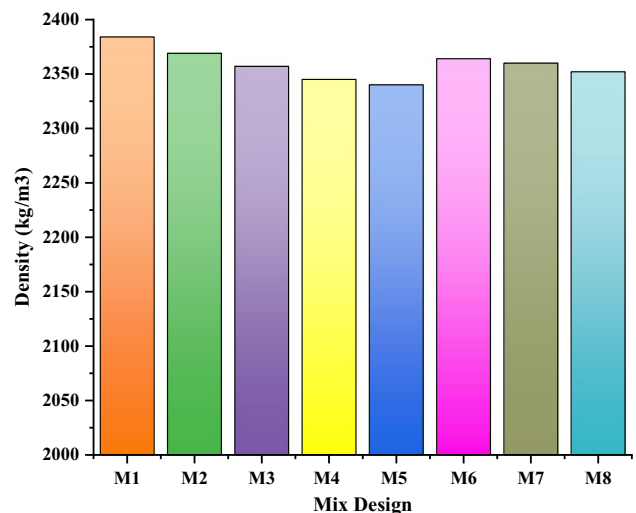
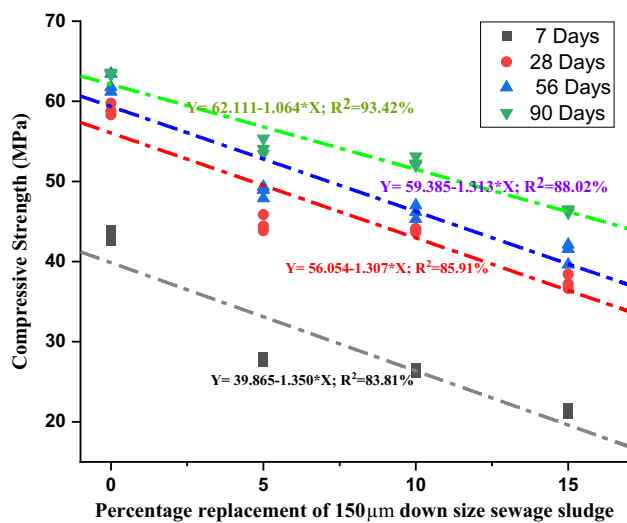


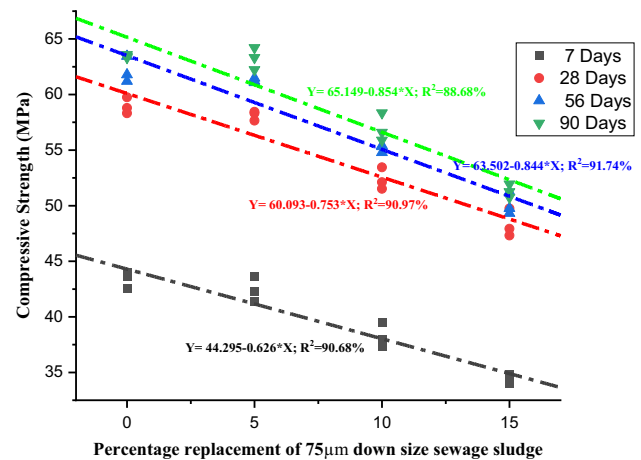
Fig. 9 Density of concrete mix at 28 days

Table 8 CS, STS, and FS of mixes at different curing ages

Concrete mix	Compressive strength (MPa)					Split tensile Strength (MPa)				Flexural strength (MPa)			
	7 day	14 day	28 day	56 day	90 day	7 day	28 day	56 day	90 day	7 day	28 day	56 day	90 day
M1	46.04	53.93	61.11	63.56	65.18	3.36	3.99	4.09	4.16	4.53	5.14	5.25	5.32
M2	43.04	45.93	58.96	62.15	64.45	3.22	3.91	4.04	4.13	4.38	5.04	5.18	5.29
M3	27.81	36.72	44.70	48.72	54.28	2.48	3.30	3.48	3.71	3.52	4.33	4.54	4.81
M4	26.37	37.42	43.90	46.18	52.45	2.40	3.26	3.37	3.64	3.44	4.29	4.41	4.73
M5	42.43	44.62	58.12	61.25	63.25	2.12	2.96	3.14	3.37	3.09	3.94	4.14	4.42
M6	38.23	43.25	52.37	55.18	56.95	3.20	3.87	4.00	4.08	4.35	5.00	5.14	5.23
M7	35.30	38.95	48.35	50.11	51.31	3.00	3.63	3.75	3.82	4.11	4.72	4.86	4.94
M8	42.43	44.62	58.12	61.25	63.25	2.86	3.46	3.54	3.59	3.93	4.52	4.61	4.67

**Fig. 10** Relationship between CS and percentage replacement level of 150 µm downsized SS

downsize contributed 1.4%, 11.17%, and 17.99% reduction for 5%, 10%, and 15% replacement levels, respectively. Jamshidi et al. (2011, 2012) [48, 79] observed that 5%, 10%, and 20% addition of dry sludge resulted in a decrease in strength by approximately 9%, 14.5%, and 28% in 28 days and 3.5%, 8%, and 20% in 90 days cured samples. It is also noted that for both the sizes, 75 µm and 150 µm sized SS, compressive strength at 90 days for 5% and 10% replacement levels is within the acceptable limits for M50 concrete. The relationship between CS and percentage replacement level is plotted, individual equations are presented in Figs. 10 and 11, and a strong relationship between percentage replacement and CS with R^2 lying between 83.81 and 93.42%.

**Fig. 11** Relationship between CS and percentage replacement level of 75 µm downsized SS

Split tensile strength

The STS results of eight mixes are illustrated in Table 8. The 28 days lowest strength of 2.96 MPa is observed in mix 5 (M5). The replacement of 150 µm downsized SS at 5%, 10%, and 15% replacement levels resulted in a considerable decrease in strength. Whereas 75 µm downsized, SS concrete samples contributed reasonably good strength than 150 µm. The relationship between STS and percentage replacement level is plotted, and individual equations are presented in Figs. 12 and 13. A direct relationship equation is plotted considering 7, 28, 56, and 90 days CS and STS and presented in Fig. 14. R^2 , a value of 0.809, indicates a correlation between them.

Flexural strength

The FS experiment results at 7, 14, 28, 56, and 90 days are illustrated in Table 8. The 28 days lowest strength of 3.94 MPa is observed for the M5 mix. The replacement of 150 µm downsized SS at 5%, 10%, and 15% replacement

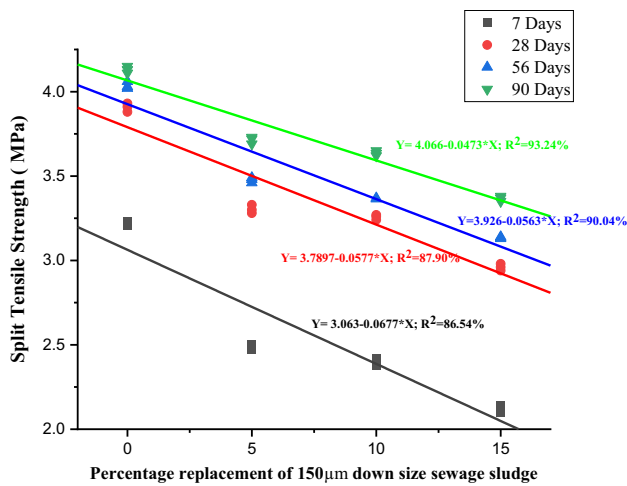


Fig. 12 Relationship between STS and percentage replacement level of 150 μ m downsized SS

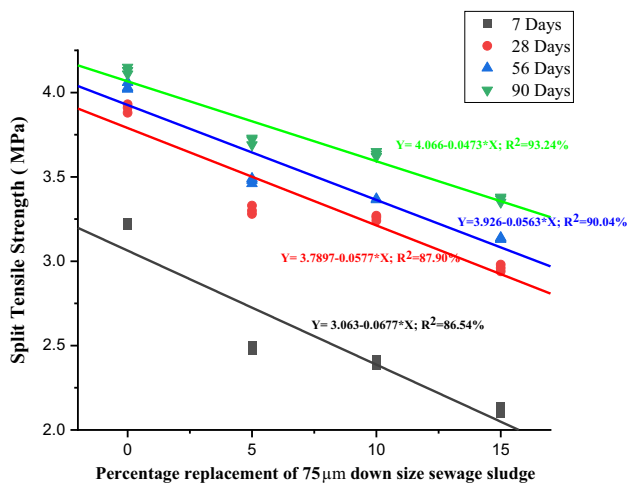


Fig. 13 Relationship between STS and percentage replacement level of 75 μ m downsized SS

levels resulted in a drastic decrease in strength. Whereas 75 μ m downsized SS exhibited higher strength than 150 μ m. The relationship between tensile strength and percentage replacement level is plotted, and individual equations are presented in Figs. 15 and 16. A direct relationship equation is plotted considering 7, 28, 56, and 90 days CS and STS and presented in Fig. 17. The R^2 value of 0.873 is observed, indicating a good correlation between them.

Modulus of elasticity (MoE)

The MoE affects reinforced concrete's safety, durability, density, and life span. The 28 days MoE of concrete specimens is calculated by applying a series of compressive stress cycles up to about 40% of the measured compressive strength and is

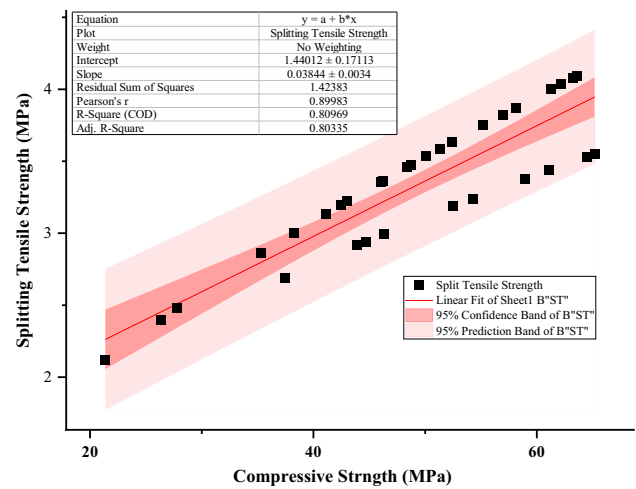


Fig. 14 Relationship between CS and STS

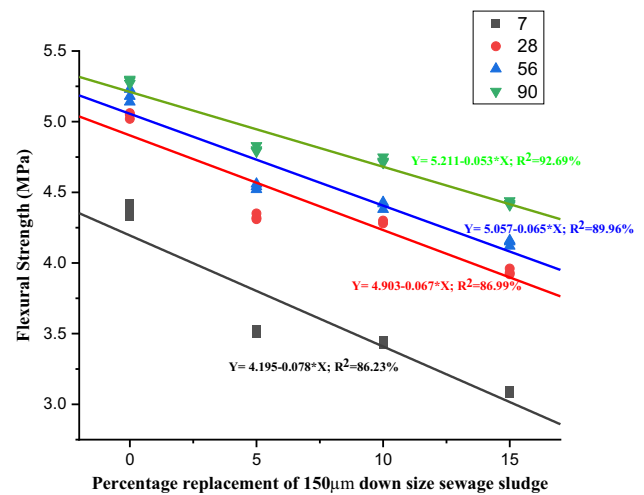


Fig. 15 Relationship between FS and percentage replacement level of 150 μ m downsized SS

presented in Fig. 18. The replacement of 150 μ m downsized SS decreased the modulus of elasticity, whereas it is similar to the control mix in the samples containing 75 μ m downsized SS. The incorporation of SS led to a decrease in MoE due to the de-densification of pore structure. A linear degradation in the value of modulus of elasticity with an increase in SS content is observed. A linear relationship between CS and MoE at 28 days is plotted in Fig. 19. A good correlation is observed with the R^2 value of 0.917.

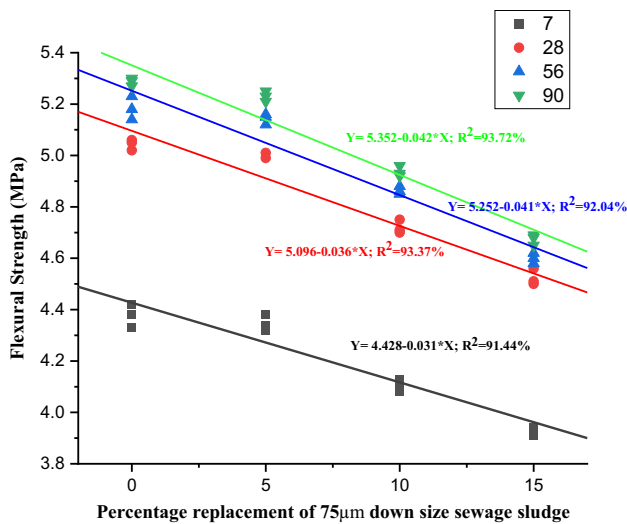


Fig. 16 Relationship between FS and percentage replacement level of 75 µm downsized SS

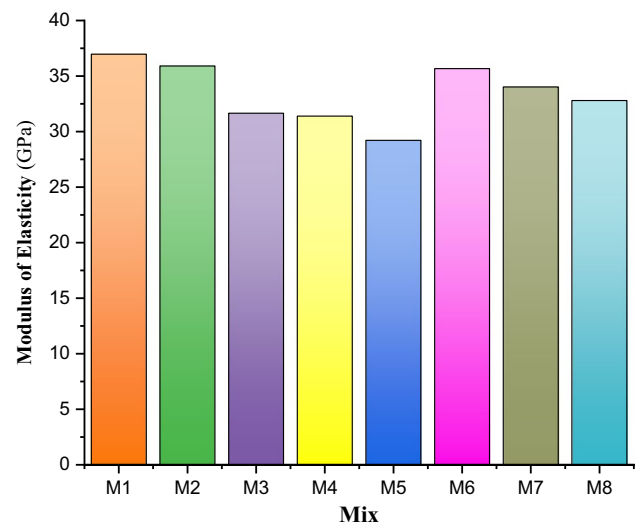


Fig. 18 MoE of mixes at 28 days

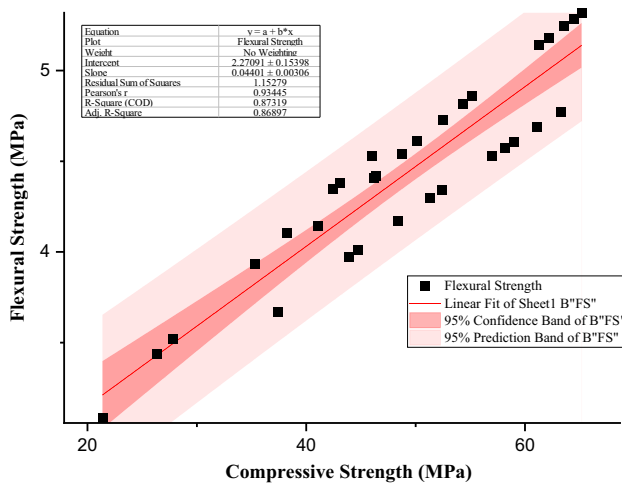


Fig. 17 Relationship between CS and FS

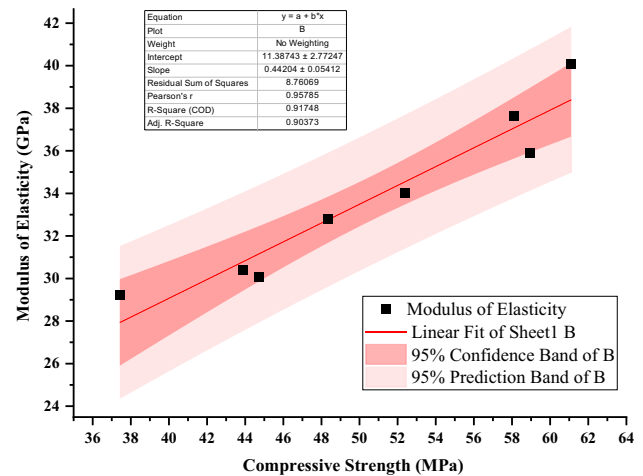


Fig. 19 Relationship between CS and MoE

Influence of sewage sludge on quality aspect of concrete

Ultrasonic pulse velocity (UPV)

The UPV test results for the mix at 28 and 90 days and correlation between UPV and CS are presented in Fig. 20. The mixes result was between 3400 and 3700 m/s, which falls under the decent to the excellent category as per IS 13111 (Part 1). The linear regression analysis has been plotted (Fig. 21) between UPV and CS. A direct relationship was obtained as y (UPV) = $2917.24 + 12.49 \cdot X$ (CS), with an R^2 value of 0.8954 showing a good correlation.

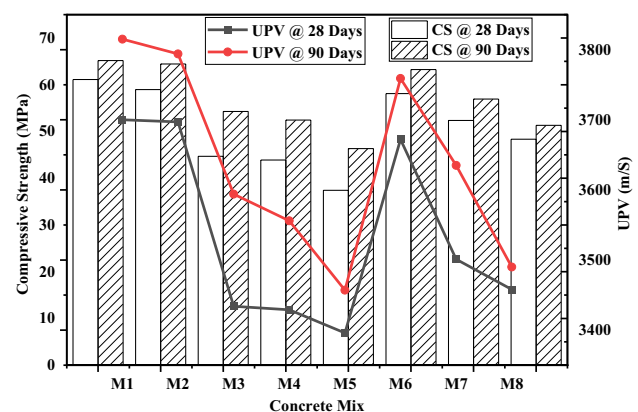


Fig. 20 Comparison between CS and UPV of the mix at 28 and 90 days

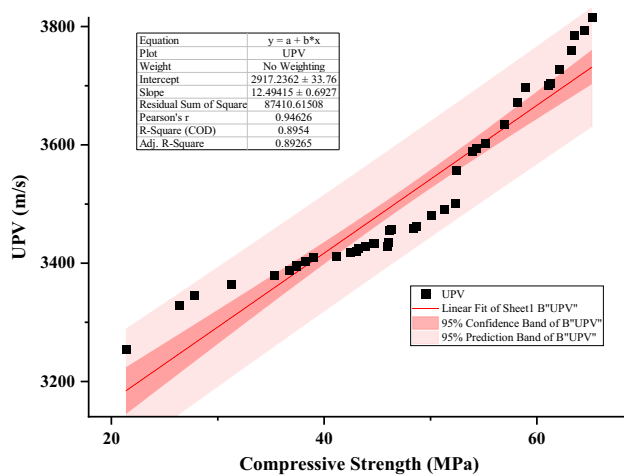


Fig. 21 Linear regression between CS and UPV

Table 9 Water absorption in percentage at 28, 56, and 90 days

	28 days	56 days	90 days
M1	4.2	3.98	3.85
M2	4.32	4.05	3.94
M3	4.48	4.26	3.99
M4	4.72	4.54	4.36
M5	4.87	4.63	4.4
M6	4.33	4.09	3.92
M7	4.39	4.12	3.96
M8	4.43	4.24	4.02

Water absorption (WA)

WA of eight mixes investigated at 28, 56, and 90 days of curing is presented in Table 9. WA decreases with an increase in curing ages in all mix specimens. An increase in SS percentage increased water absorption. However, 75 μm downsized

replacement of SS as binder material gives better results than 150 μm downsized SS particle.

Assessment of environment impact and cost implication

Using a higher dosage of supplementary cementitious material in concrete minimizes environmental impact and increases compressive strength. Cradle-to-gate EE, CE, and COST are quantified for different binder combinations. The energy consumption and CE can vary depending upon the manufacturing process, raw material, and distance from the source. Therefore, representative data from the literature were used in this study.

Carbon dioxide emission

Global warming is exacerbated by urbanization and industrialization, which leads to the depletion of natural resources, prompting scholars worldwide to consider sustainable development. As a large user of natural resources and energy, the concrete industry has significantly increased GHG emissions. According to estimates, the global population is expected to reach ten billion by 2050, resulting in increased construction and development activities and a negative impact on the environment [78, 80].

The CO_2 emission parameters were calculated in this study by calculating carbon emissions during the preparation of SCMs. According to previous studies, the carbon footprint of FA is low because it is a waste by-product of coal-burning power plants. Researchers in earlier studies state that carbon mission from FA is negligible because it is a waste by-product arising from the coal-burning power station. But in the current study, the value of 0.008 kg eq. CO_2/kg is considered for FA, as per Hammond and Jones (2011) [80, 81].

Table 10 CO_2 emission factors for sewage sludge

Material	Energy requirement for 1000 kg SS			Transport of 1000 kg SS		Total emission (kg CO ₂ /kg SS)
	Consumption (kWh)		Emission factors (kg CO ₂ / kWh)	Distance ^d	Emission factor ^e	
	Oven drying ^a	Grinding and sieving ^b				
SS (150 μm)	25	130.3	0.231	10	0.245	0.0383
SS (75 μm)	25	186.5	0.231	10	0.245	0.0513

^aEnergy utilized by oven during 24 h of drying with a utilization rate of 1041.67 W/h."

^bEnergy utilized by sieving and grinding machines."

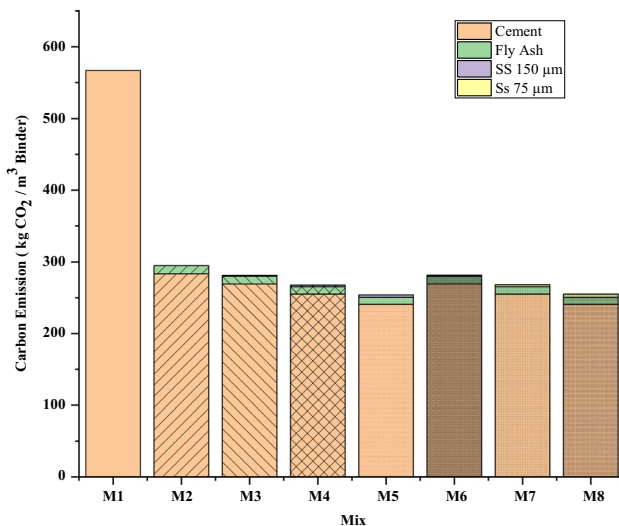
^cEmission aspect due to electricity production (DECC 2021)."

^dDistance from Municipal Treatment Plant to MIT, Manipal MAHE Campus."

^eEmission aspect of the truck used to transport the materials (DECC 2021)."

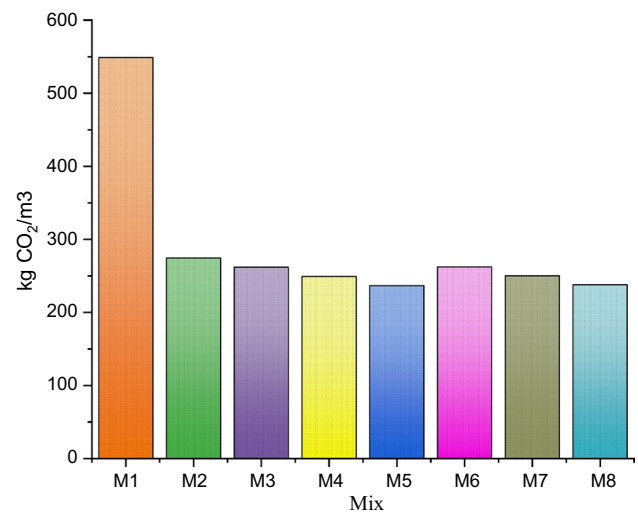
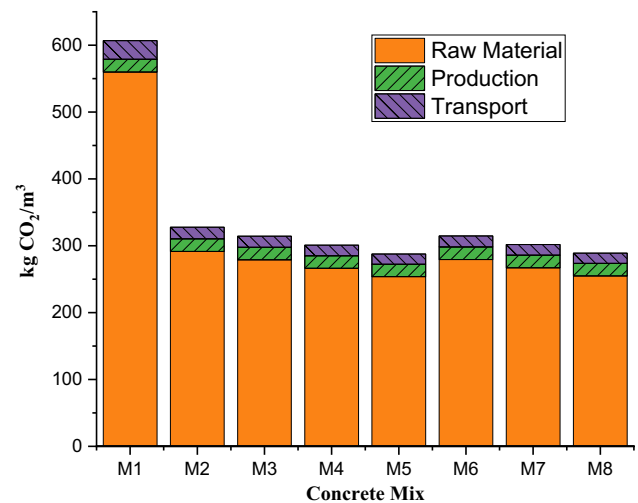
Table 11 Carbon emissions factors of raw materials

Materials	Emission factors (kg CO ₂ /kg)	References
Cement	0.951	[83]
Fly ash (FA)	0.008	[83, 84]
SS (150)	0.0383	Table 8
SS (75)	0.0513	Table 8
Coarse aggregate	0.0043	[85]
Sand	0.0026	[85]
Water	0.000196	[86]
Super plasticiser	0.944	[83, 86]

**Fig. 22** CO₂ emission of total cementitious material per mix (per m³)

Similarly, SS raw material contributes zero CO₂ emission, as it is also a by-product in municipal wastewater treatment plants [5, 82]. However, the energy utilized to improve reactivity by drying, grinding, sieving, and transport is considered for calculating carbon emission for SS and FA. According to the UK Government, conversion factors for GHG report 2021 are considered while calculating carbon emissions. Table 10 represents the calculated CO₂ emission factors for SS (150 µm) and (75 µm). The final carbon emission factors of ingredients used in concrete mixes are presented in Table 11.

The CO₂ emission of individual and total cementitious material per mix is illustrated in Figs. 22 and 23. Replacing OPC by increasing the amount of SCMs per unit volume of concrete resulted in reducing CO₂ emission of cementitious material in mixes up to 57%. The amounts of CO₂ released by each concrete mix depend upon the proportions of materials, concrete production, and raw material transport, as presented in Fig. 24. The

**Fig. 23** CO₂ emission of total cementitious material per mix (per m³)**Fig. 24** Total CO₂ emission during concrete production (kg CO₂/m³)

CO₂ emission factor was considered 0.008 kg CO₂/kg for concrete production as Kin et al. (2016) [86]. The purpose of the CO₂ emission analysis is not to achieve a mix with the lowest CO₂. Achieving a mix with less CO₂ emissions is also important, which shows acceptable mechanical properties. The results show that Mix M1 with 100% OPC has the highest emission rate of 601.24 kg CO₂/m³, while the lowest value of 293.95 kg CO₂/m³ and 295.17 kg CO₂/m³ is observed in mix M5 and M8. When SCMs were incorporated, a reduction in CO₂ emissions was observed. According to the current study result, the binder was the major contributor to CO₂ emissions at rates ranging from 80 to 90% of the total emission of 1 m³, depending upon the replacement ratio of SCMs.

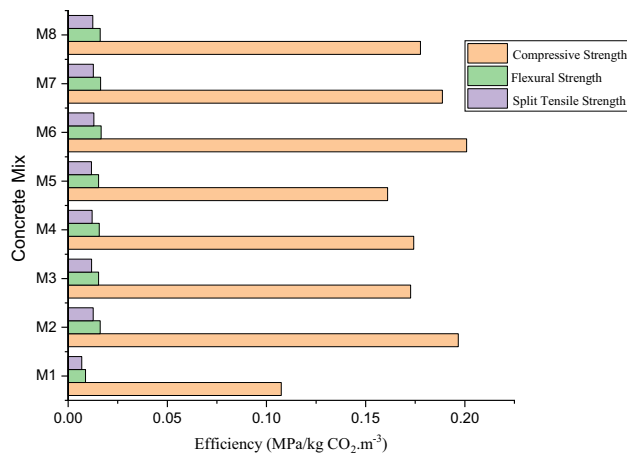


Fig. 25 Concrete eco-efficiency (compressive, flexural, and tensile) strength/CO₂ emissions

Eco-efficiency

Eco-efficiency is the ratio between 28-day mechanical strength and CO₂ equivalent emissions of the concrete mixes. Figure 25 represents the concrete eco-efficiency of eight mixes and illustrates that the mix with alternative binder materials shows better efficiency than the OPC mix. The efficiency value observed (CS) at 28 days was 0.101 MPa/kg. CO₂ m³ was in line with findings of Alnahhal et al. [86] and Stark et al. [87].

Concrete mixes with alternative binder material have shown better eco-efficiency than the control mix. The maximum eco-efficiency of 0.185 (CS), 0.0158 (FS), and 0.0123 (STS) is noticed with 75 µm downsized SS at 5% replacement.

Embodied energy and cost of blended binder

The EE of each binder material is presented in Table 12. In the current study, while comparing, the only binder material is considered since fine, and coarse aggregate content is constant for all the mix. Figure 26 shows the embodied energy of binder material of different mixes. The embodied energy of SS at 150 µm and 75 µm is calculated using available data from the literature [10, 80, 88]. It can be observed

Table 12 EE and material cost of ingredients

Material	EE (MJ/kg)	Material cost (IND Rs/kg)
Portland cement	5.5 [10, 80]	8.00
Fly ash (FA)	0.1 [81]	4.75
Sewage sludge (150 µm)	0.014 [80, 88]	1.20
Sewage sludge (75 µm)	0.0188 [80, 88]	1.60

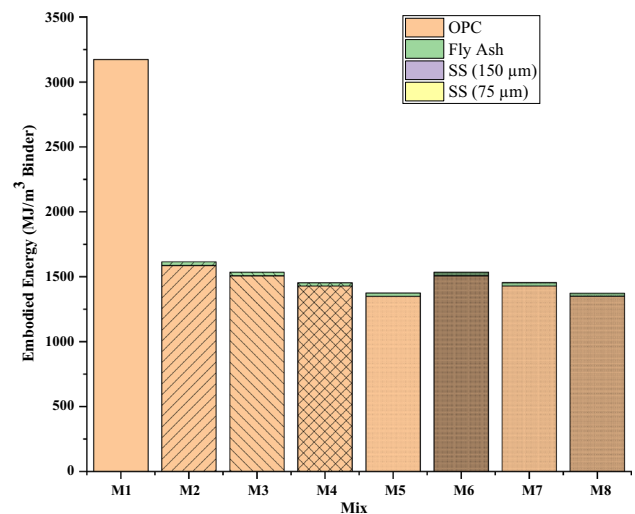


Fig. 26 Embodied energy of binder material in each mix

that a decrease in cement content and an increase in supplementary cementitious material can significantly reduce the EE and CE.

Environmental impact and binder cost per unit CS of concrete

The environmental impact quantification and binder cost per unit CS for different binder materials are calculated. The EI, CI, and binder cost index (COST) are calculated based on Eqs. 1, 2, and 3 derived with the help of an earlier study carried out by Jing Yu et al. (2021) [81].

$$EI_i \left(\frac{MJ}{m^3} / MPa \right) = \frac{\text{Embodied Energy of binder material required for } 1m^3 \text{ of concrete}}{i - \text{day compressive strength of standard concrete specimen}} \quad (1)$$

$$CI_i \left(\frac{kg \text{ CO}_2}{m^3} / MPa \right) = \frac{\text{Carbon Emission of binder material required for } 1m^3 \text{ of concrete}}{i - \text{day compressive strength of standard concrete specimen}} \quad (2)$$

$$COST_i \left(\frac{Rs}{m^3} / MPa \right) = \frac{\text{Embodied Energy of binder material required for } 1m^3 \text{ of concrete}}{i - \text{day compressive strength of standard concrete specimen}} \quad (3)$$

where i denotes the curing time in days.

The calculation results on EI, CI, and COST_i for binder material per meter cube are shown in Figs. 27, 28, and 29 at 28, 56, and 90 days. EI value of 51.93, 49.2, and 48.69 (MJ/kg)/MPa is observed for OPC mix at 28, 56, and 90 days. There is a drastic reduction in the embodied energy for the

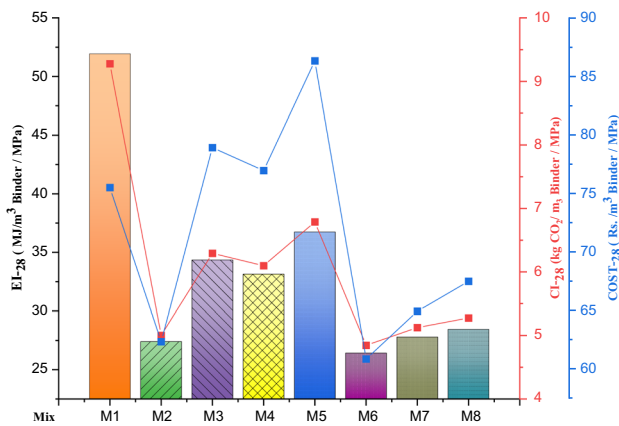


Fig. 27 Comparison of EI, CI, and COST per unit CS of the mix at 28 days

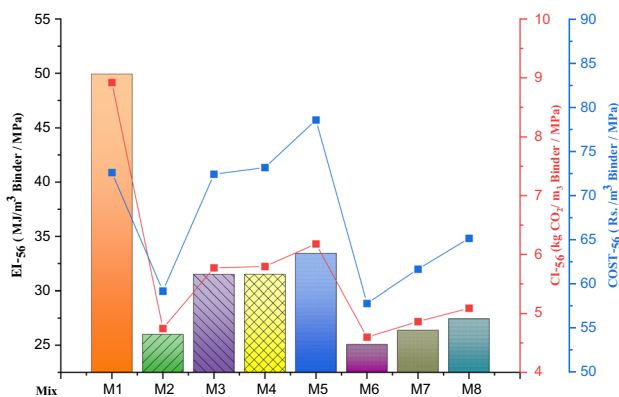


Fig. 28 Comparison of EI, CI, and COST per unit CS of the mix at 56 days

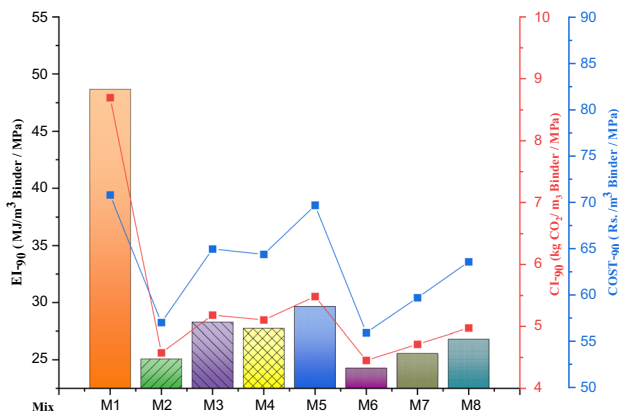


Fig. 29 Comparison of EI, CI, and COST per unit CS of the mix at 90 days

other mixes with OPC replacement. The least embodied energy index value of 26.42, 25.07, and 24.27 (MJ/kg)/MPa is observed at mix 06. The mix 7 value is on par with mix

2, which has a 50% cement replacement with FA. A similar trend is observed for 56 and 90 days.

The Carbon Emission Index value of mixes 2–8 is lesser than the control mix (M1) observed for 28, 56, and 90 days. The addition of SS resulted in the reduction of carbon emissions. At 90 days age, the trend of $COST_{90}$ is similar to $COST_{28}$ and $COST_{56}$. The $COST_{90}$ values of cement with different replacement levels of SCM are very close to each other due to significant strength development at a later stage. The mix with SS 150 μ m at 5, 10, 15, and 75 μ m at 10 and 15 replacement levels exhibited slightly lower CS than the control mix. But it has superior environmental and economic benefits by considering the environmental impact and material cost per unit strength.

Conclusion

The present study investigated the characteristics of SS, mechanical properties of concrete with different replacement levels along with carbon emissions, and embodied energy to develop sustainable and environmentally efficient concrete. A total of eight mixes with different levels of SS replacement as a binder material were cast and tested. The following main conclusions were drawn based on laboratory observations and findings.

- The main mineral components of SS are silicon dioxide, calcium, iron, and aluminum compounds. Based on the oxide content in SS, it is suitable to replace the Portland cement content in standard concrete.
- Mechanical characterizations such as CS, FS, and STP with 150 μ m were observed with a reduction in strength, whereas the strength obtained at a 5% replacement level of 75 μ m is on par with the control mix. There is no significant reduction in mechanical strength for 75 μ m SS at 5% and 10% level at 90 days.
- All of the mixes tested for UPV reported between 3400 and 3700 m/s, which falls into the decent to excellent range. A direct relationship between compressive strength and UPV was obtained as $y(UPV) = 2917.24 + 12.49 X(CS)$, with an R^2 value of 0.8954 showing a good correlation.
- Partial replacement of SS as a binder material generally affects eco-efficiency, with values similar to or higher than the control mix. The advantages of utilizing SS as a partial substitute binder material lie in reducing CO_2 emissions in making concrete and significantly reducing environmental problems caused by SS disposal.
- Incorporating SS as a binder to the concrete has a lower environmental impact, embodied energy, CO_2 emission, and cost per unit strength. But more than 10%

replacement level resulted in reducing CS, FS, and STS by 11.17%, 6.23%, and 6.99%.

In the context of sustainable development, using SS as a binder material in concrete and these findings can help the efforts to reduce the carbon footprint and embodied energy in the construction industry. It can also reduce the burden and environmental effects of disposal of SS.

Acknowledgment First of all, the authors are thankful to the Department of Civil Engineering, Manipal Institute of Technology, Manipal Academy of Higher Education, Manipal, India, for providing the necessary facilities to conduct experiments. The authors would like to thank Government Engineering College Karwar, Karnataka, Department of Collegiate and Technical Education, Palace Road, Bangalore, Karnataka, and AICTE-New Delhi for supporting our research program. The authors also thank Dr. Murari M S, Scientific Officer, DST-PURSE Program Mangalore University, for performing FE-SEM and EDS equipment. The authors would also like to acknowledge XRD and FT-IR to the central institute facility, Manipal Institute of Technology, Manipal Academy of Higher Education, Manipal, India, and the DST-FIST program, Department of Atomic and Molecular Physics, Manipal Institute of Technology, Manipal Academy of Higher Education, Manipal, India.

Funding Open access funding provided by Manipal Academy of Higher Education, Manipal.

Declarations

Conflict of interest The authors declare that they have no known competing financial interests or personal relationships that could have appeared to influence the work reported in this paper.

Ethical statement The authors declare that they have not submitted the manuscript to any other journal for simultaneous consideration. The work is original and not published elsewhere.

Open Access This article is licensed under a Creative Commons Attribution 4.0 International License, which permits use, sharing, adaptation, distribution and reproduction in any medium or format, as long as you give appropriate credit to the original author(s) and the source, provide a link to the Creative Commons licence, and indicate if changes were made. The images or other third party material in this article are included in the article's Creative Commons licence, unless indicated otherwise in a credit line to the material. If material is not included in the article's Creative Commons licence and your intended use is not permitted by statutory regulation or exceeds the permitted use, you will need to obtain permission directly from the copyright holder. To view a copy of this licence, visit <http://creativecommons.org/licenses/by/4.0/>.

References

1. Imbabi MS, Carrigan C, McKenna S (2012) Trends and developments in green cement and concrete technology. *Int J Sustain Built Environ* 1(2):194–216. <https://doi.org/10.1016/j.ijsbe.2013.05.001>
2. Flower DJM, Sanjayan JG (2007) Green house gas emissions due to concrete manufacture. *Int J Life Cycle Assess* 12(5):282–288. <https://doi.org/10.1065/lca2007.05.327>
3. Rashad AM (2015) A brief on high-volume class F fly ash as cement replacement: a guide for civil engineer. *Int J Sustain Built Environ* 4(2):278–306. <https://doi.org/10.1016/j.ijsbe.2015.10.002>
4. (Atmospheric chemist) Solomon S (2007) Intergovernmental panel on climate change., and intergovernmental panel on climate change. Working Group I. In: Climate change 2007: the physical science basis: contribution of Working Group I to the Fourth Assessment Report of the Intergovernmental Panel on Climate Change. Cambridge University Press
5. O'Brien KR, Ménaché J, O'moore LM (2009) Impact of fly ash content and fly ash transportation distance on embodied greenhouse gas emissions and water consumption in concrete
6. Chen Z, Li JS, Poon CS (2018) Combined use of sewage sludge ash and recycled glass cullet for the production of concrete blocks. *J Clean Prod* 171:1447–1459. <https://doi.org/10.1016/j.jclepro.2017.10.140>
7. Meyer C (2009) The greening of the concrete industry. *Cem Concr Compos* 31(8):601–605. <https://doi.org/10.1016/j.cemconcomp.2008.12.010>
8. Zhang Y (2014) Assessment of CO₂ emissions and cost of fly ash concrete. [Online]. Available: <https://www.researchgate.net/publication/280430859>
9. Joseph AM, Snellings R, van den Heede P, Matthys S, de Belie N (2018) The use of municipal solidwaste incineration ash in various building materials: a Belgian point of view. *Materials* 11(1):141. <https://doi.org/10.3390/ma11010141>
10. Henry CS, Lynam JG (2020) Embodied energy of rice husk ash for sustainable cement production. *Case Stud Chem Environ Eng* 2:100004. <https://doi.org/10.1016/j.csee.2020.100004>
11. Safiuddin M, West JS, Soudki KA (2010) Hardened properties of self-consolidating high performance concrete including rice husk ash. *Cem Concr Compos* 32(9):708–717. <https://doi.org/10.1016/j.cemconcomp.2010.07.006>
12. Safiuddin M, Jumaat MZ, Salam MA, Islam MS, Hashim R (2010) Utilization of solid wastes in construction materials. *Int J Phys Sci* 5(13):1952–1963. <https://doi.org/10.3844/ajessp.2013.14.24>
13. Karim MR, Zain MFM, Jamil M, Lai FC (2015) Development of a zero-cement binder using slag, fly ash, and rice husk ash with chemical activator. *Adv Mater Sci Eng*. <https://doi.org/10.1155/2015/247065>
14. Gursel AP, Maryman H, Ostertag C (2016) A life-cycle approach to environmental, mechanical, and durability properties of “green” concrete mixes with rice husk ash. *J Clean Prod* 112:823–836. <https://doi.org/10.1016/j.jclepro.2015.06.029>
15. Dyer TD, Halliday JE, Dhir KR (2011) Hydration chemistry of sewage sludge ash used as a cement component. *J Mater Civ Eng* 23(5):648–655. [https://doi.org/10.1061/\(ASCE\)MT.1943-5533.0000221](https://doi.org/10.1061/(ASCE)MT.1943-5533.0000221)
16. Xuan D, Tang P, Poon CS (2018) Effect of casting methods and SCMs on properties of mortars prepared with fine MSW incineration bottom ash. *Constr Build Mater* 167:890–898. <https://doi.org/10.1016/j.conbuildmat.2018.02.077>
17. Hu Y, Tang Z, Li W, Li Y, Tam VWY (2019) Physical-mechanical properties of fly ash/GGBFS geopolymer composites with recycled aggregates. *Constr Build Mater* 226:139–151. <https://doi.org/10.1016/j.conbuildmat.2019.07.211>
18. Boukhelkhal D, Guendouz M, Bourdot A et al (2021) Elaboration of bio-based buildingmaterials made from recycled olive core. *MRS Energy Sustain*. <https://doi.org/10.1557/s43581-021-00006-8>
19. Guendouz M, Boukhelkhal D, Bourdot A (2021) Recycling of floor tile waste as fine aggregate in flowable sand concrete. In:

- Chiba Y, Tlemçani A, Smaili A (eds) *Advances in green energies and materials technology*. Springer, Singapore
20. Mohamed G, Djamila B (2018) Properties of dune sand concrete containing coffee waste. *MATEC Web Conf* 149:01039. <https://doi.org/10.1051/mateconf/201814901039>
 21. Guendouz M, Debieb F, Boukendakdji O, Kadri EH, Bentchikou M, Soualhi H (2016) Use of plastic waste in sand concrete. *J Mater Environ Sci* 7(2):382–389
 22. Guendouz M, Boukheikh D, Bourdot A, Babachikh O, Hamadouche A (2020) The effect of ceramic wastes on physical and mechanical properties of eco-friendly flowable sand concrete. *Ceramic Materials*. IntechOpen 10(2). <https://doi.org/10.5772/intechopen.95041>
 23. Huang CH, Lin SK, Chang CS, Chen HJ (2013) Mix proportions and mechanical properties of concrete containing very high-volume of class F fly ash. *Constr Build Mater* 46:71–78. <https://doi.org/10.1016/j.conbuildmat.2013.04.016>
 24. Saravanakumar P, Dhinakaran G (2013) Strength characteristics of high-volume fly ash-based recycled aggregate concrete. *J Mater Civ Eng* 25(8):1127–1133. [https://doi.org/10.1061/\(asce\)mt.1943-5533.0000645](https://doi.org/10.1061/(asce)mt.1943-5533.0000645)
 25. Durán-Herrera A, Juárez CA, Valdez P, Bentz DP (2011) Evaluation of sustainable high-volume fly ash concretes. *Cem Concr Compos* 33(1):39–45. <https://doi.org/10.1016/j.cemconcomp.2010.09.020>
 26. Atiş CD (2005) Strength properties of high-volume fly ash roller compacted and workable concrete, and influence of curing condition. *Cem Concr Res* 35(6):1112–1121. <https://doi.org/10.1016/j.cemconres.2004.07.037>
 27. Esmeray E, Atis M (2019) Utilization of sewage sludge, oven slag and fly ash in clay brick production. *Constr Build Mater* 194:110–121. <https://doi.org/10.1016/j.conbuildmat.2018.10.231>
 28. Mukherjee S, Mandal S, and Adhikari UB (2013) Comparative study on physical and mechanical properties of high slump and zero slump high volume fly ash concrete (HVFAC)
 29. Hung HH (1997) Properties of high volume fly ash concrete
 30. Bentz DP (2014) Activation energies of high-volume fly ash ternary blends: hydration and setting. *Cem Concr Compos* 53:214–223. <https://doi.org/10.1016/j.cemconcomp.2014.06.018>
 31. Bentz DP, Ferraris CF (2010) Rheology and setting of high volume fly ash mixtures. *Cem Concr Compos* 32(4):265–270. <https://doi.org/10.1016/j.cemconcomp.2010.01.008>
 32. Jiang LH, Malhotra VM (2000) Reduction in water demand of non-air-entrained concrete incorporating large volumes of fly ash. *Cem Concr Res* 30(11):1785–1789. [https://doi.org/10.1016/S0008-8846\(00\)00397-5](https://doi.org/10.1016/S0008-8846(00)00397-5)
 33. Dunstan DJ, Thomas MRH, Cripwell MDA, Harrison JB (1992) Investigation into the long-term in-situ performance of high fly ash content concrete used for structural application. In: Fly ash, silica fume, slag & normal pozzolans in concrete. In: FProceedings fourth international conference, Istanbul, Turkey, pp 1–20
 34. Sivasundaram V, Carette GG, Malhotra VM (1990) Long-term strength development of high-volume fly ash concrete. *Cem Concr Compos* 12(4):263–270
 35. Bouzoubaâ N, Zhang MH, Malhotra VM (2000) Laboratory-produced high-volume fly ash blended cements: compressive strength and resistance to the chloride-ion penetration of concrete. *Cem Concr Res* 30(7):1037–1046. [https://doi.org/10.1016/S0008-8846\(00\)00299-4](https://doi.org/10.1016/S0008-8846(00)00299-4)
 36. Mateo-Sagasta J, Raschid-Sally L, Thebo A (2015) Global wastewater and sludge production, treatment, and use. In: Drechsel P, Qadir M, Wichelns D (eds) *Wastewater: economic asset in an urbanizing world*. Springer, Dordrecht, pp 15–38
 37. Singh V, Phuleria HC, Chandel MK (2020) Estimation of energy recovery potential of sewage sludge in India: waste to watt approach. *J Clean Prod*. <https://doi.org/10.1016/j.jclepro.2020.122538>
 38. Yan P et al (2017) Net-zero-energy model for sustainable wastewater treatment. *Environ Sci Technol* 51(2):1017–1023. <https://doi.org/10.1021/acs.est.6b04735>
 39. Meena RS (2016) Environmental accounting for municipal solid waste management: a case study of Udaipur city (Rajasthan) in the faculty of earth science by faculty of earth science
 40. Lundin M, Olofsson M, Pettersson GJ, Zetterlund H (2004) Environmental and economic assessment of sewage sludge handling options. *Resour Conserv Recycl* 41(4):255–278. <https://doi.org/10.1016/j.resconrec.2003.10.006>
 41. Chakraborty S, Jo BW, Jo JH, Baloch Z (2017) Effectiveness of sewage sludge ash combined with waste pozzolanic minerals in developing sustainable construction material: an alternative approach for waste management. *J Clean Prod* 153:253–263. <https://doi.org/10.1016/j.jclepro.2017.03.059>
 42. Chen YC, Kuo J (2016) Potential of greenhouse gas emissions from sewage sludge management: a case study of Taiwan. *J Clean Prod* 129:196–201. <https://doi.org/10.1016/j.jclepro.2016.04.084>
 43. Fontes CMA, Toledo Filho RD, Barbosa MC (2017) Sewage sludge ash (SSA) in high performance concrete: characterization and application. *Rev IBRACON Estrut Mater* 9(6):989–1006. <https://doi.org/10.1590/s1983-41952016000600009>
 44. Nakić D, Vouk D, Štirmer N, Serdar M (2018) Management of sewage sludge-new possibilities involving partial cement replacement. *Gradjevinar* 70(4):277–286. <https://doi.org/10.14256/JCE.2164.2017>
 45. Mariscal C, Valls S, Yagu A, Va E (2004) Physical and mechanical properties of concrete with added dry sludge from a sewage treatment plant. *Cem Concr Res* 34:2203–2208. <https://doi.org/10.1016/j.cemconres.2004.02.004>
 46. Baskar R, Begum KMMS, Sundaram S (2006) Characterization and re use of textile effluent treatment plant waste sludge in bricks. *J Univ Chem Technol Metall* 41:473–478
 47. Patel H, Pandey S (2012) Evaluation of physical stability and leachability of Portland Pozzolona Cement (PPC) solidified chemical sludge generated from textile wastewater treatment plants. *J Hazard Mater* 207–208:56–64. <https://doi.org/10.1016/j.jhazmat.2011.05.028>
 48. Jamshidi M (2011) Application of sewage dry sludge as fine aggregate in concrete. *J Environ Stud* 37(59):4–6. <https://doi.org/10.1164/ajrcem.161.6.9909098>
 49. IS 8112:2013 (2013) Ordinary Portland cement, 43 grade—specification
 50. Mladenović A, Hamler S, Zupančič N (2017) Environmental characterisation of sewage sludge/paper ash-based composites in relation to their possible use in civil engineering. *Environ Sci Pollut Res* 24(1):1030–1041. <https://doi.org/10.1007/s11356-016-7843-2>
 51. O’Kelly BC (2006) Geotechnical properties of municipal sewage sludge. *Geotech Geol Eng* 24(4):833–850. <https://doi.org/10.1007/s10706-005-6611-8>
 52. Kadir AA, Salim NSA, Sarani NA, Rahmat NAI, Abdullah MMAB (2017) Properties of fired clay brick incorporating with sewage sludge waste. *AIP Conf Proc*. <https://doi.org/10.1063/1.5002344>
 53. Gu C, Ji Y, Zhang Y, Yang Y, Liu J, Ni T (2021) Recycling use of sulfate-rich sewage sludge ash (SR-SSA) in cement-based materials: assessment on the basic properties, volume deformation, and microstructure of SR-SSA blended cement pastes. *J Clean Prod*. <https://doi.org/10.1016/j.jclepro.2020.124511>
 54. Mladenović A, Von E, Pav K (2014) Sewage sludge/biomass ash based products for sustainable construction. *J Clean Prod*. <https://doi.org/10.1016/j.jclepro.2013.12.034>
 55. Amin ShK, Abdel Hamid EM, El-Sherbiny SA, Sibak HA, Abadir MF (2018) The use of sewage sludge in the production of ceramic

- floor tiles. HBRC J 14(3):309–315. <https://doi.org/10.1016/j.hbrcj.2017.02.002>
56. Amminudin AL, Ramadhansyah PJ, Doh SI, Mangi SA, Mohd Haziman WI (2020) Effect of dried sewage sludge on compressive strength of concrete. IOP Conf Ser Mater Sci Eng. <https://doi.org/10.1088/1757-899X/712/1/012042>
 57. Zhan BJ, Poon CS (2015) Study on feasibility of reutilizing textile effluent sludge for producing concrete blocks. J Clean Prod 101:174–179. <https://doi.org/10.1016/j.jclepro.2015.03.083>
 58. 1995 BS EN 196: Part 3 (1995) Methods of testing cement. Part 3: determination of setting time and soundness. no May, p 10
 59. I. Standard (2008) IS 180086-1982: specification for reaffirmed 2004 moulds for use in tests of cement and concrete. vol 20, no 2. DOI: [https://doi.org/10.1016/0006-2952\(71\)90086-4](https://doi.org/10.1016/0006-2952(71)90086-4)
 60. IS 516-1959 (2004) (Reaffirmed 2004): method of tests for strength of concrete
 61. I. Standard (2019) IS 10262: 2019, Concrete mix proportioning—licensed. Indian Standards, no January 2019
 62. Jagadish A, Rao B, Nayak G, Kamath M (2021) Influence of nano-silica on the microstructural and mechanical properties of high-performance concrete of containing EAF aggregate and processed quarry dust. 2021, [Online]. Available: <https://doi.org/10.1016/j.conbuildmat.2021.124392>
 63. C191-19, "ASTM C191-19," (2019) Standard test methods for time of setting of hydraulic cement by Vicat needle. pp 1–8, 2019. DOI: <https://doi.org/10.1520/C0191-19.2>
 64. C187-16, "ASTM C187-16," (2011) Standard test method for amount of water required for normal consistency of hydraulic cement paste. pp 4–6. DOI: <https://doi.org/10.1520/C0187-16.2>
 65. C618-19, "ASTM C618-19," (2019) Standard specification for coal fly ash and raw or calcined natural pozzolan for use in concrete. pp 1–5. DOI: <https://doi.org/10.1520/C0618-19.2>
 66. C1437-20, "ASTM C1437-20," (2020) Standard test method for flow of hydraulic cement mortar. pp 4–5. DOI: <https://doi.org/10.1520/C1437-20.2>
 67. B. of Indian Standards, "IS 5816 (1999): Method of test splitting tensile strength of concrete
 68. IS-13311-1(1992), "IS 13311-1 (1992): Method of non-destructive testing of concrete, part 1: ultrasonic pulse velocity
 69. BS:1881-1983: Part 122 (2009) BS 1881-122-(1983)-testing concrete-method for determination of water absorption. British Standard, vol 3, no 2014, pp 420–457
 70. IS 1199: 1959 (2004) IS 1199-1959: Indian Standard Methods of sampling and analysis of concrete. Indian Standards, pp 1199–1959
 71. B. Standard (1997) BS 1881-114: 1983: Testing concrete—part 114: methods for determination of density of hardened concrete. no December 1997
 72. Mirza J, Mirza MS, Roy V, Saleh K (2002) Basic rheological and mechanical properties of high-volume fly ash grouts. Constr Build Mater 16(6):353–363. [https://doi.org/10.1016/S0950-0618\(02\)00026-0](https://doi.org/10.1016/S0950-0618(02)00026-0)
 73. Ma F, Sha A, Yang P, Huang Y (2016) The greenhouse gas emission from portland cement concrete pavement construction in China. Int J Environ Res Public Health. <https://doi.org/10.3390/ijerph13070632>
 74. Marthong C (2012) Effect of fly ash additive on concrete properties. Int J Eng Res Appl (IJERA) 2:1986–1991
 75. Mourtada Rabie G (2016) Using of wastewater dry and wet sludge in concrete mix. J Civ Environ Eng 06(01):1–7. <https://doi.org/10.4172/2165-784X.1000209>
 76. Şahmaran M, Yaman İÖ, Tokyay M (2009) Transport and mechanical properties of self consolidating concrete with high volume fly ash. Cem Concr Compos 31(2):99–106. <https://doi.org/10.1016/j.cemconcomp.2008.12.003>
 77. Rabie GM, El-Halim HA, Rozaik EH (2019) Influence of using dry and wet wastewater sludge in concrete mix on its physical and mechanical properties. Ain Shams Eng J 10(4):705–712. <https://doi.org/10.1016/j.asej.2019.07.008>
 78. Dezhampannah S, Nikbin I, Charkhtab S, Fakhimi F, Mehdipour S, Mohebbi R (2020) Environmental performance and durability of concrete incorporating waste tire rubber and steel fiber subjected to acid attack. J Clean Prod 268:122216. <https://doi.org/10.1016/j.jclepro.2020.122216>
 79. Jamshidi M, Jamshidi A, Mehrdadi N, Pacheco-Torgal F (2012) Mechanical performance and capillary water absorption of sewage sludge ash concrete (SSAC). Int J Sustain Eng 5(3):228–234. <https://doi.org/10.1080/19397038.2011.642020>
 80. Hammond G, Jones C, Lowrie F, Tse P (2011) Building Services Research and Information Association., and University of Bath. Embodied carbon : the inventory of carbon and energy (ICE). BSRIA
 81. Yu J, Wu HL, Mishra DK, Li G, Leung CK (2021) Compressive strength and environmental impact of sustainable blended cement with high-dosage limestone and calcined clay (LC2). J Clean Prod. <https://doi.org/10.1016/j.jclepro.2020.123616>
 82. Müller HS, Haist M, Vogel M (2014) Assessment of the sustainability potential of concrete and concrete structures considering their environmental impact, performance and lifetime. Constr Build Mater 67:321–337. <https://doi.org/10.1016/j.conbuildmat.2014.01.039>
 83. Turner LK, Collins FG (2013) Carbon dioxide equivalent (CO₂-e) emissions: a comparison between geopolymers and OPC cement concrete. Constr Build Mater 43:125–130. <https://doi.org/10.1016/j.conbuildmat.2013.01.023>
 84. Habert G, Denarié E, Šajna A, Rossi P (2013) Lowering the global warming impact of bridge rehabilitations by using ultra high performance fibre reinforced concretes. Cem Concr Compos 38:1–11. <https://doi.org/10.1016/j.cemconcomp.2012.11.008>
 85. Kim TH, Chae CU, Kim GH, Jang HJ (2016) Analysis of CO₂ emission characteristics of concrete used at construction sites. Sustainability (Switzerland). <https://doi.org/10.3390/su8040348>
 86. Alnahhal MF, Alengaram UJ, Jumaat MZ, Abutaha F, Alqedra MA, Nayaka RR (2018) Assessment on engineering properties and CO₂ emissions of recycled aggregate concrete incorporating waste products as supplements to Portland cement. J Clean Prod 203:822–835. <https://doi.org/10.1016/j.jclepro.2018.08.292>
 87. Stark K, Plaza E, Hultman B (2006) Phosphorus release from ash, dried sludge and sludge residue from supercritical water oxidation by acid or base. Chemosphere 62:827e832. <https://doi.org/10.1016/j.chemosphere.2005.04.069>
 88. Ding A et al (2021) Life cycle assessment of sewage sludge treatment and disposal based on nutrient and energy recovery: a review. Sci Total Environ. <https://doi.org/10.1016/j.scitotenv.2020.144451>